

RESEARCH LETTER

10.1002/2017GL076150

Key Points:

- Summertime ozone air quality in the eastern United States is related to sea surface temperature anomalies mainly in the eastern Pacific
- El Niño can increase ozone in the middle and south Atlantic states but decrease ozone in the south central by altering atmospheric circulation
- Niño 1 + 2 can be used to predict the summertime ozone air quality in the eastern U.S. by as much as 4 months in advance

Supporting Information:

- Supporting Information S1

Correspondence to:

L. Shen,
lshen@fas.harvard.edu

Citation:

Shen, L., & Mickley, L. J. (2017). Effects of El Niño on summertime ozone air quality in the eastern United States. *Geophysical Research Letters*, 44, 12,543–12,550. <https://doi.org/10.1002/2017GL076150>

Received 23 OCT 2017

Accepted 7 DEC 2017

Accepted article online 13 DEC 2017

Published online 29 DEC 2017

©2017. The Authors.

This is an open access article under the terms of the Creative Commons Attribution-NonCommercial-NoDerivs License, which permits use and distribution in any medium, provided the original work is properly cited, the use is non-commercial and no modifications or adaptations are made.

Effects of El Niño on Summertime Ozone Air Quality in the Eastern United States

Lu Shen¹  and Loretta J. Mickley¹ 

¹John A. Paulson School of Engineering and Applied Sciences, Harvard University, Cambridge, MA, USA

Abstract We investigate the effect of El Niño on maximum daily 8 h average surface ozone over the eastern United States in summer during 1980–2016. El Niño can influence the extratropical climate through the propagation of stationary waves, leading to (1) reduced transport of moist, clean air into the middle and southern Atlantic states and greater subsidence, reduced precipitation, and increased surface solar radiation in this region, as well as (2) intensified southerly flow into the south central states, which here enhances flux of moist and clean air. As a result, each standard deviation increase in the Niño 1 + 2 index is associated with an increase of 1–2 ppbv ozone in the Atlantic states and a decrease of 0.5–2 ppbv ozone in the south central states. These influences can be predicted 4 months in advance. We show that U.S. summertime ozone responds differently to eastern-type El Niño events compared to central-type events.

1. Introduction

The El Niño–Southern Oscillation (ENSO) is the dominant interannual mode of variability in tropical meteorology. ENSO also influences regional weather in the United States. For example, ENSO winters are usually characterized by warm weather over Canada and the northern United States, as well as cold and wet weather in the southern United States (e.g., Yu, Zou et al., 2012; Yu & Zou, 2013). In summer, the magnitude of ENSO reduces, and ENSO teleconnections to midlatitudes also weaken (Neelin et al., 2000). Despite this weakening, ENSO can still significantly change summertime synoptic circulations as well as local meteorology in the United States (e.g., Liang et al., 2015; Wang et al., 2012; Weaver et al., 2009). Because high surface ozone concentrations in most industrial regions are tied to increased temperatures, reduced wind speeds, clear skies, and stagnant weather (e.g., Fiore et al., 2015; Shen et al., 2015, 2016), it follows that ENSO may also influence ozone air quality in the United States. More importantly, surface ozone concentrations reach a maximum in summer over most U.S. regions, and any perturbation in ozone concentrations during this season could have potentially large impacts on public health. In this study, we investigate and quantify the effects of ENSO on summertime ozone air quality in the eastern United States.

To our knowledge, only a few studies have examined the relationships between ENSO and U.S. ozone air quality, and none have focused on summertime ozone. Using a combination of observations and modeling simulations, Lin et al. (2015) found that enhanced stratosphere-troposphere exchange following La Nina could increase springtime surface ozone concentrations by as much as 30 ppbv on days with surface ozone above 70 ppbv versus days below 60 ppbv in the Intermountain West. Using Niño 3.4 index to represent ENSO variability, Xu et al. (2017) reported that every standard deviation increase in Niño 3.4 decreases surface ozone by 1.4–1.7 ppb in the fall in the southeastern United States when ENSO is in a developing phase. In contrast, when ENSO is in a decaying phase, springtime ozone decreases by 1.0–1.4 ppbv in the western United States (Xu et al., 2017). However, Niño 3.4 mainly characterizes sea surface temperature (SST) variability in the central tropical Pacific. In fact, there are two types of El Niño: (1) the central Pacific (CP) type with SST anomalies near the International Date Line and (2) the eastern Pacific (EP) type with anomalies mainly in eastern Pacific (e.g., Kao & Yu, 2009; Yu & Kao, 2007; Yu & Kim, 2011). In this study, we demonstrate that U.S. ozone air quality in summer is more closely related to sea surface temperature variability in the eastern tropical Pacific Ocean, with Niño 1 + 2 a better metric than the more commonly used Niño 3.4 to characterize the ENSO influence.

ENSO is likely to have effects on the U.S. summertime ozone through altering regional meteorology and synoptic circulations. Previous studies (e.g., Bunkers et al., 1996; Trenberth & Guillemot, 1996; Ting & Wang, 1997; Wang et al., 2012) have quantified the dependence of the U.S. summer precipitation on tropical Pacific SST variability. Wang et al. (2012) revealed that summer precipitation anomalies vary according to

El Niño phase. In the developing and decaying phase of an EP El Niño, precipitation is above normal in the Midwest and Great Plains but below normal in states along the Gulf Coast. During CP El Niño summers, precipitation displays a tripole pattern, with positive anomalies in the deep south and far north as well as negative anomalies in the central United States. Liang et al. (2015) found that the influence on the summertime Great Plains low-level jet depends on El Niño type, with an increase in EP-type years and a decrease in CP-type years. In the upper troposphere, tropical warming induced by El Niño is associated with positive 200 hPa geopotential height anomalies over the tropics, as well as a wave train extending from the tropics to the extratropics (e.g., Kumar & Hoerling, 2003; Wang et al., 2012); such teleconnections likely vary among different El Niño types. As surface ozone concentrations are tied to local weather conditions as well as to synoptic circulation (Shen et al., 2015), these relationships imply a link between June–July–August (JJA) ozone air quality in the United States and El Niño, which is not well investigated.

In this study, we seek to identify the influence of El Niño on U.S. summertime ozone air quality. We build on our previous work (Shen et al., 2015; Shen, Mickley et al., 2017) by first regressing detrended, mean JJA maximum daily 8 h average (MDA8) ozone across the eastern U.S. onto local meteorological variables from 1980 to 2016. We then apply empirical orthogonal functions (EOFs) to decompose the resulting ozone residuals. This process enables us to focus on the signals arising from atmospheric teleconnections, including the influence of El Niño. We then investigate the physical mechanisms linking El Niño and the observed ozone pattern and evaluate whether present climate models can simulate these mechanisms. Finally, we compare the relationship of U.S. summertime ozone with different ENSO indices, including Niño 1 + 2, Niño 3, Niño 3.4, Niño 4, EP-type, and CP-type El Niño.

2. Data and Methods

We obtain the 1980–2016 daily maximum 8 h average (MDA8) ozone from the EPA Air Quality System (AQS, <http://www.epa.gov/ttn/airs/airsaqs/>), and then interpolate onto $2.5^\circ \times 2.5^\circ$ resolution by averaging all observations within each grid cell. We also compare the results in AQS with those in the EPA Clean Air Status and Trends Network (CASTNET, <http://epa.gov/castnet/>) from 1990 to 2016. Unlike the AQS network, CASTNET sites are mainly located in the rural regions with less anthropogenic influence (Cooper et al., 2012). The meteorological data used in this study consist of surface air temperature, surface solar radiation, total cloud fraction, sea level pressure (SLP), vertical velocity (omega), horizontal wind speed, and geopotential height from the National Centers for Environmental Prediction Reanalysis 1 with a $2.5^\circ \times 2.5^\circ$ grid resolution (Kalnay et al., 1996). For precipitation, we rely on the NOAA Climate Prediction Center Unified Gauge-Based Analysis of Daily Precipitation (Chen et al., 2008; Xie et al., 2007). We also use the NOAA Extended Reconstructed sea surface temperatures (SSTs, ERSST v4). The Niño 1 + 2, Niño 3, Niño 4, and Niño 3.4 indices are obtained from NOAA (<https://www.esrl.noaa.gov/psd/data/climateindices/list/>). The EP and CP El Niño indices are defined using a regression-EOF analysis (Kao & Yu, 2009; Yu & Tae Kim, 2010), as downloaded from <https://www.ess.uci.edu/~yu/2OSC/>. Detrended data and anomalies are obtained by subtracting the 7 year moving averages.

We also evaluate the skill of present climate models in simulating the effects of El Niño on U.S. regional climate. To that end, we analyze the meteorological output from an ensemble of 25 models participating in the Atmospheric Model Intercomparison Project (AMIP), part of the Coupled Model Intercomparison Project, phase 5. Only the first ensemble member of each model is used in our analysis. The AMIP models use observed SSTs and sea ice as boundary conditions (Gates et al., 1999).

3. Identifying the Impact of El Niño on U.S. Ozone

Summertime surface ozone concentrations are highly associated with local meteorological conditions (e.g., Fiore et al., 2015; Shen et al., 2016; Shen & Mickley, 2017), and the ozone signal arising from El Niño or other atmospheric teleconnections may be much smaller than that from local weather variability. By removing the effects of stronger signals, EOF analysis of the residuals may uncover patterns related to weaker signals. As a first step, we calculate the ozone residuals using a multivariate linear regression model to correlate the seasonal mean JJA MDA8 ozone in grid cells across the eastern United States from 1980 to 2016 with local meteorological variables, including surface air temperature, specific humidity, and north-south and east-west wind speeds. The regression coefficients for each variable can be found in Figure S1 in the supporting

EOFs of JJA ozone residuals with SSTs/teleconnections

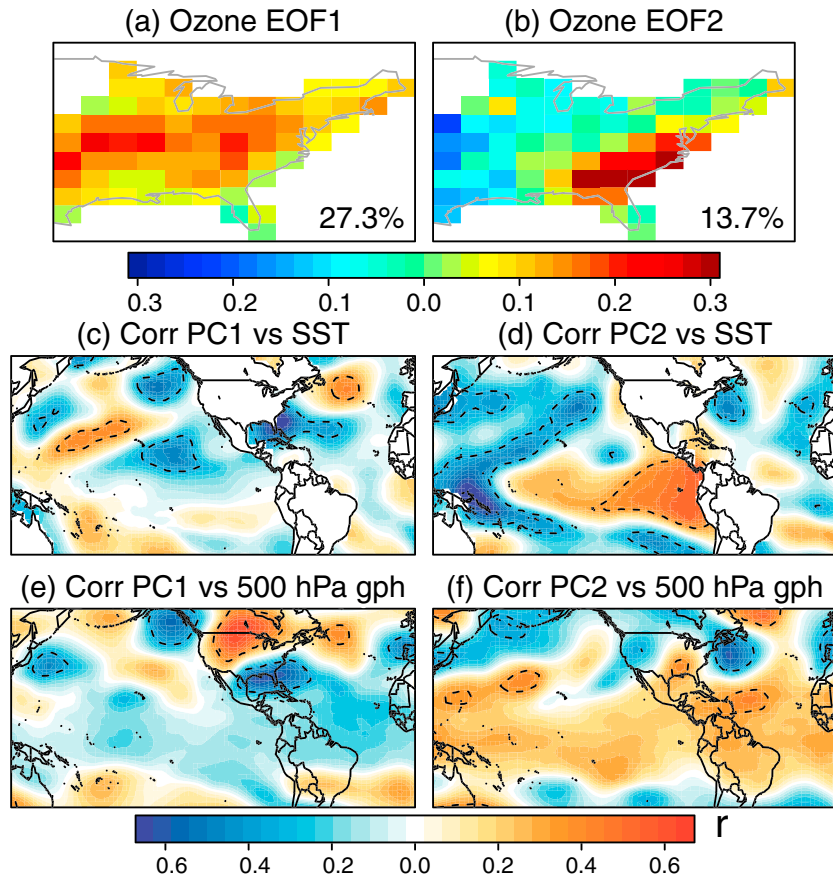


Figure 1. (a and b) Empirical orthogonal function (EOF) loadings of JJA seasonal mean ozone residuals from 1980 to 2016 after removing the effects of surface air temperature, specific humidity, and north-south and east-west wind speeds. (c and d) Correlations between the principal components time series for the first and second mode (PC1 and PC2) with sea surface temperatures. (e and f) Same as in Figures 1c and 1d but for the 500 hPa geopotential heights. All data are detrended by removing the 7 year moving average. The dashed contour lines enclose regions in which the correlations reach statistical significance ($p < 0.05$).

information. We find that this linear regression model performs as well as a polynomial one given the relatively short history of ozone (Figure S2). We then apply EOFs to decompose the seasonal variability of these ozone residuals. This approach yields patterns of ozone variability that can be regressed onto observed meteorological variables, such as SST and 500 hPa geopotential heights, revealing the causes of the weaker signals in ozone variability.

The first EOF pattern (EOF1), which explains 27.3% of the total variance in the ozone residuals or 12.3% in the original ozone anomaly, displays a swath of positive anomaly across the eastern United States (Figure 1a). We find that EOF1 is associated with a tripole SST pattern in the Pacific, with negative correlations in the north-east Pacific over both high latitudes (40°N–60°N) and low latitudes (10°N–20°N), as well as positive correlations in the central Pacific (Figure 1c). EOF1 is also anticorrelated with SSTs in the Gulf of Mexico and adjacent to the east coast (Figure 1c). In the midtroposphere, EOF1 is linked to a wave train extending across the midlatitudes from the western Pacific to northern Atlantic, with a ridge in 500 hPa geopotential heights over southern Canada and the Intermountain west and a trough over the southeast and Gulf of Mexico (Figure 1e). This atmospheric teleconnection can reduce jet wind speeds across the eastern United States, which, in turn, promotes more stagnant weather and enhanced ozone concentrations at the surface in this region (e.g., Shen et al., 2015). The correlation coefficient between the time series of EOF1 and Pacific North America (PNA) pattern is insignificant, indicating that this teleconnection pattern is independent of PNA.

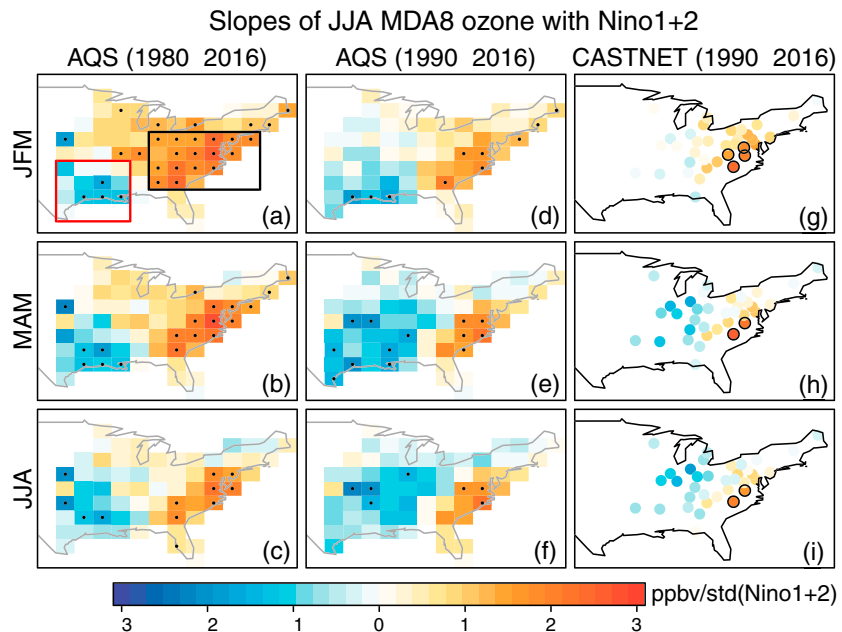


Figure 2. Slope of JJA AQS ozone with standardized Niño 1 + 2 index in (a) Jan-Feb-Mar, (b) Mar-Apr-May, and (c) Jun-Jul-Aug for 1980–2016. (d–f) Same as in Figures 2a–2c but for the 1990–2016 timeframe. (g–i) Same as in Figures 2d–2f but using the ozone observations in CASTNET. All data are detrended by subtracting the 7 year moving averages. The grid boxes with statistically significant correlations ($p \leq 0.1$) are stippled in Figures 2a–2f or circled in Figures 2g–2i. The black and red rectangles in Figure 2a are used to define the ozone dipole pattern as discussed in Figure 54.

We also find that the second EOF pattern (EOF2), which explains 13.7% of the total variance in the ozone residuals or 6.0% in the original ozone anomaly, exerts a significant east-west contrast in the eastern United States, with positive anomalies in the south Atlantic States and negative anomalies in the southern Great Plains (Figure 1b). Figure 1d shows that EOF2 is coincident in time with the EP type of El Niño, with positive correlations in the eastern Pacific and negative correlations in the western Pacific, so we use Niño 1 + 2 index (averaged SST in the eastern tropical Pacific, 90°W–80°W, 0–10°S) to characterize this pattern. In removing the effects of four local meteorological variables before conducting this EOF analysis, we may have also inadvertently removed some of the El Niño influences on these variables. To address this uncertainty, we repeat the EOF analysis, removing the effects of different combinations of local meteorological variables. We find for all experiments the EOF2 patterns are consistent and significantly correlated with Niño 1 + 2 (Figure S3). The relationship of EOF2 with 500 hPa geopotential heights is characterized by a trough in the western Atlantic, adjacent to North America (Figure 1f). We also find positive correlations in the tropical regions as well as a wave train extending from the tropics to the extratropics (Figure 1f), a typical atmospheric response to El Niño (Kumar & Hoerling, 2003). Since these correlations are insignificant over most regions at the 95% confidence level, we next examine the relationship of El Niño and surface ozone by analyzing direct correlations between them.

Figures 2a–2c show the slopes of seasonal mean JJA MDA8 ozone and standardized Niño 1 + 2 index in the seasons leading up to and including summer over the 1980–2016 time period. In all seasons, we find positive slopes in the middle and southern Atlantic States and negative slopes in the south central states, resembling the east-west dipole pattern in EOF2 of the ozone residuals (Figure 1b). The region correlating significantly with the January-February-March (JFM) and March-April-May (MAM) Niño 1 + 2 indexes (Figures 2a and 2b) is much larger than that using the JJA index (Figure 2c), suggesting that there is a delay in the response of ozone air quality in the eastern United States to tropical Pacific warming. This result implies that we can predict this ozone pattern as much as 4 months in advance, with implications for air quality management. In the more recent 1990–2016 timeframe, we find a similar dipole pattern in the slopes of ozone and Niño 1 + 2 index using AQS (Figures 2d–2f) and CASTNET (Figures 2g–2i) observations, suggesting that the effect of El Niño on U.S. ozone that we identify is robust. On average, every standard deviation increase in the Niño 1 + 2 index is associated with an increase of 1–2 ppbv ozone in the middle and southern Atlantic states and a decrease of 0.5–2 ppbv ozone in the south central states.

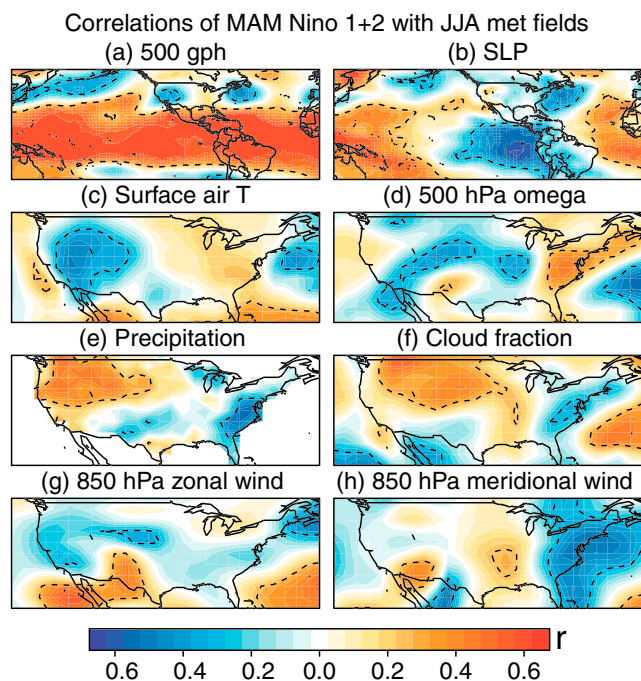


Figure 3. Correlation of MAM Niño 1 + 2 with JJA atmospheric teleconnections, including (a) 500 hPa geopotential heights and (b) sea level pressures, from 1980 to 2016. (c–h) Same as in Figures 3a and 3b but for other meteorological variables over the United States. The positive values denote subsidence in Figure 3d, eastward wind in Figure 3g, and northward wind in Figure 3h. All data are detrended by removing the 7 year moving average. The dashed contour lines enclose regions in which the correlations reach statistical significance ($p < 0.10$).

We also regress this ozone dipole pattern, defined as the difference in mean JJA MDA8 ozone over the middle and southern Atlantic states (black rectangle, Figure 2a) versus that over the south central states (red rectangle), with different El Niño indices in the lead-lag months, including Niño 1 + 2 ($0^{\circ}\text{--}10^{\circ}\text{S}$, $90^{\circ}\text{W--}80^{\circ}\text{W}$), Niño 3 ($5^{\circ}\text{N--}5^{\circ}\text{S}$, $150^{\circ}\text{W--}90^{\circ}\text{W}$), Niño 3.4 ($5^{\circ}\text{N--}5^{\circ}\text{S}$, $170^{\circ}\text{W--}120^{\circ}\text{W}$), and Niño 4 ($5^{\circ}\text{N--}5^{\circ}\text{S}$, $160^{\circ}\text{E--}150^{\circ}\text{W}$). Among these indices, Niño 1 + 2 shows the highest correlations across nearly all lead-lag times (Figure S4), indicating that it is the best metric to characterize the influence of ENSO on summertime ozone air quality in the east. The especially high correlation for Niño 1 + 2 at a lead time of 4 months suggests a delayed response of ozone air quality to tropical Pacific warming. This delay time is more than the time required for atmospheric Rossby waves to propagate from the tropics to the extratropics, indicating that other terrestrial or ocean processes are needed to explain this delay. Other examples of similarly lagged relationships include the association of wintertime El Niño with springtime warming in the northern tropical Atlantic (e.g., Alexander & Scott, 2002; Wang et al., 2017) and the link between springtime warming in the northern tropical Atlantic with enhanced JJA ozone anomalies in the eastern United States (Shen & Mickley, 2017). Previous studies have also shown that the U.S. summertime temperature is related to soil moisture (e.g., Mo, 2003) or the precipitation deficit (e.g., McKinnon et al., 2016) in spring. Such processes may help explain the gap between JFM El Niño and JJA ozone anomalies.

By checking the anomalous ozone pattern in typical El Niño years, we provide additional insight into the east-west dipole pattern of surface ozone associated with EOF2 (Figures 1b and 2). Figure S5a displays the time series of JFM and MAM Niño 1 + 2 index from 1980 to 2016. We find five years characterized by high Niño 1 + 2 index: 1983, 1987, 1992, 1998, and 2016. This sequence is consistent with the fact the EP El Niño has become

less frequent since early this century (e.g., Yu & Kim, 2011), a change that may be linked to extratropical forcing associated with the North Pacific Oscillation (Di Lorenzo et al., 2010; Kim et al., 2012; Yu, Lu et al., 2012). Figure S5b shows the patterns of anomalous JJA ozone in each of these five years. As seen from the figure, the dipole pattern with high ozone in the south Atlantic States and low ozone in the south central is a clear feature in 1983, 1987, 1998, and 2016. The magnitude of these ozone anomalies has declined in more recent years, likely due in part to reduced anthropogenic emissions and decreasing ozone concentrations under the Clean Air Act (e.g., Cooper et al., 2012) and in part to the relatively weak El Niño signal in 2016. However, we observe anomalously low ozone concentrations in summer 1992. The eastern United States experienced a relatively cool summer that year (1°C below normal) as a result of aerosol radiative forcing following the 1991 eruption of Mount Pinatubo (e.g., Kirchner et al., 1999; Parker et al., 1996). We hypothesize that this cooling effect may have overridden the effects of El Niño on surface ozone that summer, leading to reduced ozone in the East. With regard to the other El Niño summers, we find relative changes of ozone concentrations up to $\pm 15\%$ in 1983, 1987, and 1998 and $\pm 5\%$ in 2016 (Figure S6).

4. Physical Mechanisms for the Relationship of El Niño and U.S. MDA8 Ozone

A warm tropical Pacific can trigger diabatic heating in the atmosphere and influence the extratropics through stationary wave propagation. Figure 3a shows the mapped correlation coefficients of JJA 500 hPa geopotential heights with MAM El Niño 1 + 2 from 1980 to 2016, displaying positive correlations in the tropics and a wave chain extending from the tropics to the extratropics, consistent with previous studies (e.g., Kumar & Hoerling, 2003; Wang et al., 2012). This atmospheric teleconnection also features a trough over the Atlantic Ocean just offshore of the eastern United States (Figure 3a). Figure 3b reveals a dipole pattern in sea level pressure (SLPs) in the tropical Pacific that forms in response to El Niño warming in the eastern tropical Pacific. Consistent with the teleconnection trough aloft (Figure 3a), SLPs in the western Atlantic decrease (Figure 3b).

We find that local meteorological weather in summer also shows a strong dependence on MAM El Niño. Enhanced El Niño 1 + 2 index is associated with significantly cooler temperatures in the Intermountain West but only slight warming in the eastern United States (Figure 3c). El Niño also appears to induce subsidence in the East, leading to reduced precipitation as well as decreasing cloud fraction there (Figures 3d–3f). We find that El Niño has little influence on the zonal wind speed in the lower troposphere (Figure 3g) but increases the southerly wind speed across the south central states, which brings clean air from the Gulf of Mexico into the continent (Figure 3h). In contrast, the decreasing SLP in the western Atlantic (Figure 3b) results in decreased southerly wind speeds in the eastern coastal regions (Figure 3h), reducing the flux of clean ocean air into this region. These responses in meridional wind speeds to enhancements in EP El Niño are consistent with those identified by Liang et al. (2015), who compared the influences of EP and CP El Niño conditions on the Great Plains low level jet. We also show that these meteorological impacts are consistent if we use the Niño 1 + 2 index during JFM instead of MAM (Figure S7).

We next investigate whether present climate models can capture the observed links between El Niño and regional summertime weather variability in the United States using AMIP models, which as noted above use observed SSTs as boundary conditions (Gates et al., 1999). In general, these models can simulate the hemispheric teleconnection patterns similar to those observed, but they have difficulty capturing the El Niño influence on summertime weather in the eastern United States (Figure S8). More details can be found in Text S1 and Figures S8–S11 in the supporting information.

5. Relationship of U.S. Summertime Ozone With Other El Niño Indices

El Niño can be defined using SST anomalies in different tropical Pacific regions. Figures S12a–S12d compare the slopes of seasonal mean JJA MDA8 ozone with different El Niño indices, including Niño 1 + 2, Niño 3, Niño 3.4, and Niño 4, in the seasons leading up to and including summer over 1980–2016. For all these indices, we find positive slopes in the middle and southern Atlantic States and negative slopes in the south central states, with Niño 1 + 2 yielding the strongest correlations with U.S. summertime ozone. To understand the stronger link of ozone with Niño 1 + 2, we examine the response of U.S. ozone to La Niña events. Figure S13 displays the ozone anomalies in five years characterized by low Niño 3.4 index, all categorized as CP La Niña events (Yuan & Yan, 2013). The plots reveal a mixed picture, with, for example, strong ozone decreases in 1989 but increases in 2011. The Niño 1 + 2 index, however, is relatively insensitive to CP La Niña events during 1980–2016, as suggested by Figure S5a. Thus, we find that this index is a better metric than Niño 3.4 to characterize the influence of ENSO on U.S. summertime ozone air quality over the past three decades.

Since atmospheric circulation patterns vary between EP and CP El Niño years (Liang et al., 2015; Wang et al., 2012; Yu, Zou et al., 2012), we also examine the relationship of U.S. summertime ozone with these two types of El Niño (Figures S12e and S12f). Because EP El Niño mainly reflects the SST variability in the Niño 1 + 2 region, it is not surprising that it displays similar dipole patterns of correlations with U.S. summertime ozone, compared to those patterns using Niño 1 + 2 (Figures S12a and S12e). The mapped correlation coefficients of meteorological variables with EP El Niño are also consistent with these obtained by using Niño 1 + 2 (Figures 3 and S14). Since the effects of Niño 1 + 2 have been removed when defining the CP El Niño (Kao & Yu, 2009; Yu & Tae Kim, 2010), we find the MAM CP El Niño is associated a reversed dipole pattern of ozone (Figure S12f), with decreased surface JJA ozone in the middle and southern Atlantic states and increased ozone in the south central states. This pattern is related to decreased subsidence and greater cloud fraction in the Atlantic States, as well as reduced southerly ocean flow into the south central states (Figure S15), both associated with CP El Niño.

6. Conclusions

This study investigates the effect of El Niño–Southern Oscillation (ENSO) on maximum daily 8 h average (MDA8) surface ozone over the eastern United States in summer (June–August, JJA) from 1980 to 2016. Using Niño 1 + 2 to characterize ENSO variability, we find that ENSO can induce a dipole pattern in surface ozone concentrations, with increased ozone in the middle and southern Atlantic states and decreased ozone in the south central states. This dipole pattern should be a robust feature, which we obtained through three independent methods: (1) the second empirical orthogonal function (EOF) pattern of JJA ozone residuals after removing the effects of local meteorology, (2) correlation of JJA ozone with Niño 1 + 2 index in the

seasons leading up to and including summer, and (3) JJA ozone anomalies in typical El Niño years. On average, every standard deviation increase in the Niño 1 + 2 index is associated with an increase of 1–2 ppbv ozone in the middle and southern Atlantic states and a decrease of 0.5–2 ppbv ozone in the south central states. We find that variation in surface ozone can be predicted as much as 4 months in advance, which would be useful for air quality management. We also show that the summertime ozone responds differently to the EP and CP El Niño events. However, for reasons that are unclear, U.S. summertime ozone is relatively insensitive to central Pacific La Niña events; this may explain why Niño 1 + 2 is a better metric than Niño 3.4 to characterize the ENSO influence on U.S. summertime ozone.

El Niño influences the extratropical climate and ozone air quality in the eastern United States through the propagation of stationary waves. This teleconnection can lead to low SLP anomalies in the western Atlantic and greater subsidence, less precipitation, and increased solar radiation in the middle and southern Atlantic States, enhancing ozone concentrations there. In the south central states, southerly flow intensifies in El Niño years, which, in turn, enhances the flux the moisture and clean air into the continent, decreasing ozone concentrations in this region. On average, models participating in the Atmospheric Model Intercomparison Project (AMIP) fail to simulate the influence of El Niño on JJA meteorological variability in the eastern United States, implying that such freely running chemistry-climate models may not be able to capture the observed effects of El Niño on U.S. air quality. In response to greenhouse-gas warming, extreme El Niño events may occur more frequently (Cai et al., 2015), highlighting the need to consider its influence when planning future air quality management.

Acknowledgments

This work was supported by the National Aeronautics and Space Administration (NASA Air Quality Applied Sciences Team and NASA-MAP NNX13AO08G), the National Institute of Environmental Health Sciences (NIH R21ES022585), and the Environmental Protection Agency (EPA-83575501 and EPA-83587201). It has not been formally reviewed by EPA. The views expressed in this document are solely those of the authors and do not necessarily reflect those of the agency. EPA does not endorse any products or commercial services mentioned in this publication. All data used in this study can be accessed via <https://doi.org/10.7910/DVN/NJ2XGL>.

References

- Alexander, M., & Scott, J. (2002). The influence of ENSO on air-sea interaction in the Atlantic. *Geophysical Research Letters*, 29(14), 1701. <https://doi.org/10.1029/2001GL014347>
- Bunkers, M. J., Miller, J. R. Jr., & DeGaetano, A. T. (1996). An examination of El Niño-La Niña related precipitation and temperature anomalies across the Northern Plains. *Journal of Climate*, 9(1), 147–160. [https://doi.org/10.1175/1520-0442\(1996\)009%3C0147:AEOENN%3E2.0.CO;2](https://doi.org/10.1175/1520-0442(1996)009%3C0147:AEOENN%3E2.0.CO;2)
- Cai, W., Santoso, A., Wang, G., Yeh, S. W., An, S. I., Cobb, K. M., ... Wu, L. (2015). ENSO and greenhouse warming. *Nature Climate Change*, 5(9), 849–859. <https://doi.org/10.1038/nclimate2743>
- Chen, M., Shi, W., Xie, P., Silva, V. B. S., Kousky, V. E., Wayne Higgins, R., & Janowiak, J. E. (2008). Assessing objective techniques for gauge-based analyses of global daily precipitation. *Journal of Geophysical Research*, 113, D04110. <https://doi.org/10.1029/2007JD009132>
- Cooper, O. R., Gao, R.-S., Tarasick, D., Leblanc, T., & Sweeney, C. (2012). Long-term ozone trends at rural ozone monitoring sites across the United States, 1990–2010. *Journal of Geophysical Research*, 117, D22307. <https://doi.org/10.1029/2012JD018261>
- Di Lorenzo, E., Cobb, K. M., Furtado, J. C., Schneider, N., Anderson, B. T., Bracco, A., ... Vimont, D. J. (2010). Central Pacific El Niño and decadal climate change in the North Pacific. *Nature Geoscience*, 3(11), 762–765. <https://doi.org/10.1038/ngeo984>
- Fiore, A. M., Naik, V., & Leibensperger, E. M. (2015). Air quality and climate connections. *Journal of the Air & Waste Management Association*, 65(6), 645–685. <https://doi.org/10.1080/10962247.2015.1040526>
- Gates, W. L., Boyle, J. S., Covey, C., Dease, C. G., Doutriaux, C. M., Drach, R. S., ... Williams, D. N. (1999). An overview of the results of the Atmospheric Model 511 Intercomparison Project (AMIP I). *Bulletin of the American Meteorological Society*, 80(1), 29–55. [https://doi.org/10.1175/1520-0477\(1999\)080%3C0029:AOTRO%3E2.0.CO;2](https://doi.org/10.1175/1520-0477(1999)080%3C0029:AOTRO%3E2.0.CO;2)
- Kalnay, E., Kanamitsu, M., Kistler, R., Collins, W., Deaven, D., Gandin, L., ... Joseph, D. (1996). The NCEP/NCAR 40-year reanalysis project. *Bulletin of the American Meteorological Society*, 77(3), 437–471. [https://doi.org/10.1175/1520-0477\(1996\)077%3C0437:TNYRP%3E2.0.CO;2](https://doi.org/10.1175/1520-0477(1996)077%3C0437:TNYRP%3E2.0.CO;2)
- Kao, H.-Y., & Yu, J.-Y. (2009). Contrasting eastern-Pacific and central-Pacific types of ENSO. *Journal of Climate*, 22(3), 615–632. <https://doi.org/10.1175/2008JCLI2309.1>
- Kim, S. T., Yu, J. Y., Kumar, A., & Wang, H. (2012). Examination of the two types of ENSO in the NCEP CFS model and its extratropical associations. *Monthly Weather Review*, 140(6), 1908–1923. <https://doi.org/10.1175/MWR-D-11-00300.1>
- Kirchner, I., Stechnikov, G. L., Graf, H.-F., Robock, A., & Antuna, J. C. (1999). Climate model simulation of winter warming and summer cooling following the 1991 Mount Pinatubo volcanic eruption. *Journal of Geophysical Research*, 104(D16), 19,039–19,055. <https://doi.org/10.1029/1999JD900213>
- Kumar, A., & Hoerling, M. (2003). The nature and causes for the delayed atmospheric response to el Niño. *Journal of Climate*, 16(9), 1391–1403. <https://doi.org/10.1175/1520-0442-16.9.1391>
- Liang, Y.-C., Yu, J.-Y., Lo, M.-H., & Wang, C. (2015). The changing influence of El Niño on the Great Plains low-level jet. *Atmospheric Science Letters*, 16(4), 512–517. <https://doi.org/10.1002/asl.590>
- Lin, M., Fiore, A. M., Horowitz, L. W., Langford, A. O., Oltmans, S. J., Tarasick, D., & Rieder, H. E. (2015). Climate variability modulates western U.S. ozone air quality in spring via deep stratospheric intrusions. *Nature Communications*, 6, 7105. <https://doi.org/10.1038/ncomms8105>
- McKinnon, K. A., Rhines, A., Tingley, M. P., & Huybers, P. (2016). Long-lead predictions of eastern United States hot days from Pacific sea surface temperatures. *Nature Geoscience*, 9(5), 389–394. <https://doi.org/10.1038/ngeo2687>
- Mo, K. C. (2003). Ensemble canonical correlation prediction of surface temperature over the United States. *Journal of Climate*, 16(11), 1665–1683. [https://doi.org/10.1175/1520-0442\(2003\)016%3C1665:ECCPOS%3E2.0.CO;2](https://doi.org/10.1175/1520-0442(2003)016%3C1665:ECCPOS%3E2.0.CO;2)
- Neelin, J. D., Jin, F.-F., & Syu, H. H. (2000). Variations in ENSO phase locking. *Journal of Climate*, 13(14), 2570–2590. [https://doi.org/10.1175/1520-0442\(2000\)013%3C2570:VIEPL%3E2.0.CO;2](https://doi.org/10.1175/1520-0442(2000)013%3C2570:VIEPL%3E2.0.CO;2)
- Parker, D. E., Wilson, H., Jones, P. D., Christy, J. R., & Folland, C. K. (1996). The impact of Mount Pinatubo on worldwide temperatures. *International Journal of Climatology*, 75, 487–497.
- Shen, L., & Mickley, L. J. (2017). Influence of large-scale climate patterns on summertime U.S. ozone: A seasonal predictive model for air quality management. *Proceedings of the National Academy of Sciences of the United States of America*, 114(10), 2491–2496. <https://doi.org/10.1073/pnas.1610708114>

- Shen, L., Mickley, L. J., & Gilleland, E. (2016). Impact of increasing heat waves on U.S. ozone episodes in the 2050s: Results from a multimodel analysis using extreme value theory. *Geophysical Research Letters*, *43*(8), 4017–4025. <https://doi.org/10.1002/2016GL068432>
- Shen, L., Mickley, L. J., & Murray, L. (2017). Influence of 2000–2050 climate change on particulate matter in the United States: Results from a new statistical model. *Atmospheric Chemistry and Physics*, *17*(6), 4355–4367. <https://doi.org/10.5194/acp-17-4355-2017>
- Shen, L., Mickley, L. J., & Tai, A. P. K. (2015). Influence of synoptic patterns on surface ozone variability over the eastern United States from 1980 to 2012. *Atmospheric Chemistry and Physics*, *15*(19), 10,925–10,938. <https://doi.org/10.5194/acp-15-10925-2015>
- Ting, M., & Wang, H. (1997). Summertime U.S. precipitation variability and its relation to Pacific sea surface temperature. *Journal of Climate*, *10*(8), 1853–1873. [https://doi.org/10.1175/1520-0442\(1997\)010%3C1853:SUSPVA%3E2.0.CO;2](https://doi.org/10.1175/1520-0442(1997)010%3C1853:SUSPVA%3E2.0.CO;2)
- Trenberth, K. E., & Guillemot, C. J. (1996). Physical processes involved in the 1988 drought and 1993 floods in North America. *Journal of Climate*, *9*(6), 1288–1298. [https://doi.org/10.1175/1520-0442\(1996\)009%3C1288:PIITD%3E2.0.CO;2](https://doi.org/10.1175/1520-0442(1996)009%3C1288:PIITD%3E2.0.CO;2)
- Wang, H., Kumar, A., Wang, W., & Jha, B. (2012). U.S. summer precipitation and temperature patterns following the peak phase of El Niño. *Journal of Climate*, *25*(20), 7204–7215. <https://doi.org/10.1175/JCLI-D-11-00660.1>
- Wang, L., Yu, J. Y., & Paek, H. (2017). Enhanced biennial variability in the Pacific due to Atlantic capacitor effect: The influence of ENSO on air-sea interaction in the Atlantic. *Nature Communications*, *8*, 14887. <https://doi.org/10.1038/ncomms14887>
- Weaver, S. J., Schubert, S., & Wang, H. (2009). Warm season variations in the low-level circulation and precipitation over the Central United States in observations, AMIP simulations, and idealized SST experiments. *Journal of Climate*, *22*(20), 5401–5420. <https://doi.org/10.1175/2009JCLI2984.1>
- Xie, P., Yatagai, A., Chen, M., Hayasaka, T., Fukushima, Y., Liu, C., & Yang, S. (2007). A gauge-based analysis of daily precipitation over East Asia. *Journal of Hydrometeorology*, *8*(3), 607–626. <https://doi.org/10.1175/JHM583.1>
- Xu, L., Yu, J.-Y., Schnell, J. L., & Prather, M. J. (2017). The seasonality and geographic dependence of ENSO impacts on U.S. surface ozone variability. *Geophysical Research Letters*, *44*, 3420–3428. <https://doi.org/10.1002/2017GL073044>
- Yu, J.-Y., & Kao, H.-Y. (2007). Decadal changes of ENSO persistence barrier in SST and ocean heat content indices: 1958–2001. *Journal of Geophysical Research*, *112*, D13106. <https://doi.org/10.1029/2006JD007654>
- Yu, J.-Y., Lu, M.-M., & Kim, S. T. (2012). A change in the relationship between tropical central Pacific SST variability and the extratropical atmosphere around 1990. *Environmental Research Letters*, *7*(3), 034025. <https://doi.org/10.1088/1748-9326/7/3/034025>
- Yu, J.-Y., & Tae Kim, S. (2010). Three evolution patterns of Central-Pacific El Niño. *Geophysical Research Letters*, *37*, L08706. <https://doi.org/10.1029/2010GL042810>
- Yu, J. Y., & Kim, S. T. (2011). Identifying the types of major El Niño events since 1870. *International Journal of Climatology*, *33*, 2105–2112. <https://doi.org/10.1088/1748-9326/8/1/014019>
- Yu, J.-Y., & Zou, Y. (2013). The enhanced drying effect of Central-Pacific El Niño on U.S. winter. *Environmental Research Letters*, *8*(1), 014019. <https://doi.org/10.1088/1748-9326/8/1/014019>
- Yu, J.-Y., Zou, Y., Kim, S. T., & Lee, T. (2012). The changing impact of El Niño on U.S. winter temperatures. *Geophysical Research Letters*, *39*, L15702. <https://doi.org/10.1029/2012GL052483>
- Yuan, Y., & Yan, H. (2013). Different types of La Niña events and different responses of the tropical atmosphere. *Chinese Science Bulletin*, *58*(3), 406–415. <https://doi.org/10.1007/s11434-012-5423-5>